Cell. Mol. Life Sci. (2015) 72:1209–1225
DOI 10.1007/s00018-014-1745-6

Cellular and Molecular Life Sciences

RESEARCH ARTICLE

ARTC1-mediated ADP-ribosylation of GRP78/BiP: a new player in endoplasmic-reticulum stress responses

Gaia Fabrizio · Simone Di Paola · Annalisa Stilla · Monica Giannotta · Carmen Ruggiero · Stephan Menzel · Friedrich Koch-Nolte · Michele Sallese · Maria Di Girolamo

Received: 8 April 2014 / Revised: 23 September 2014 / Accepted: 25 September 2014 / Published online: 8 October 2014

Abstract Protein mono-ADP-ribosylation is a reversible post-translational modification of cellular proteins. This scheme of amino-acid modification is used not only by bacterial toxins to attack host cells, but also by endogenous ADP-ribosyltransferases (ARTs) in mammalian cells. These latter ARTs include members of three different families of proteins: the well characterised arginine-specific ecto-enzymes (ARTCs), two sirtuins, and some members of the poly(ADP-ribose) polymerase (PARP/ARTD) family. In the present study, we demonstrate that human ARTC1 is localised to the endoplasmic reticulum (ER), in contrast to the previously characterised ARTC proteins, which are typical GPI-anchored ecto-enzymes. Moreover, using the "*macro* domain" cognitive binding module to identify ADP-ribosylated proteins, we show here that the ER luminal chaperone GRP78/BiP (glucose-regulated protein of 78 kDa/immunoglobulin heavy-chain-binding protein) is a cellular target of human ARTC1 and hamster ARTC2. We further developed a procedure to visualise ADP-ribosylated proteins using immunofluorescence. With this approach, in cells overexpressing ARTC1, we detected staining of the ER that co-localises with GRP78/BiP, thus confirming that this modification occurs in living cells. In line with the key role of GRP78/BiP in the ER stress response system, we provide evidence here that ARTC1 is activated during the ER stress response, which results in acute ADP-ribosylation of GRP78/BiP paralleling translational inhibition. Thus, this identification of ARTC1 as a regulator of GRP78/BiP defines a novel, previously unsuspected, player in GRP78-mediated ER stress responses.

Keywords ADP-ribosyltransferase · Post-translational modification · ADP-ribosylation ·

G. Fabrizio and S. Di Paola contributed equally to this manuscript.

Electronic supplementary material The online version of this article (doi:10.1007/s00018-014-1745-6) contains supplementary material, which is available to authorized users.

G. Fabrizio · S. Di Paola · A. Stilla · M. Di Girolamo (✉)
Laboratory of G-Protein-mediated Signalling, Department of Cellular and Translational Pharmacology, Mario Negri Sud Foundation, Via Nazionale 8/A, 66030 Santa Maria Imbaro, CH, Italy
e-mail: mdigirolamo@negrisud.it

M. Giannotta · C. Ruggiero · M. Sallese
Genomic Approaches to Membrane Traffic Unit, Department of Cellular and Translational Pharmacology, Mario Negri Sud Foundation, Via Nazionale, 8/A, 66030 Santa Maria Imbaro, CH, Italy

S. Menzel · F. Koch-Nolte
Institute of Immunology, University Medical Centre Hamburg-Eppendorf, Martinist 52, 20246 Hamburg, Germany

Present Address:
S. Di Paola
Telethon Institute of Genetics and Medicine, Via Pietro Castellino 111, 80131 Naples, Italy

Present Address:
M. Giannotta
Unit of Vascular Biology, The FIRC Institute of Molecular Oncology Foundation, Milan, Italy

Present Address:
C. Ruggiero
Associated International Laboratory (LIA) NEOGENEX CNRS, University of Nice Sophia Antipolis, Institut de Pharmacologie Moléculaire et Cellulaire, CNRS, 660 route des Lucioles, Sophia Antipolis, 06560 Valbonne, France

Macro domain · Endoplasmic reticulum · GRP78/BiP · Dithiothreitol · Thapsigargin · Chaperone

Abbreviations

ART	ADP-ribosyltransferase
CHO cells	Chinese hamster ovary cells
DTT	Dithiothreitol
ER	Endoplasmic reticulum
GST	Glutatione S-transferase
HeLa cells	Human cervix adenocarcinoma cells

Introduction

Post-translational modifications of cellular proteins by ADP-ribosylation have been associated with a number of cellular processes. In addition to the nuclear role of the poly-ADP-ribose polymerase PARP1, which regulates cellular pathways that are critical for genome stability and mitosis [1–5], mono-ADP-ribosylation reactions have been shown to be important in mitochondrial activity, stress-responses, intracellular trafficking, and cell signalling [6–11]. The mono-ADP-ribosylation reaction consists of the transfer of a single ADP-ribose moiety from βNAD^+ to a specific amino-acid residue of various cellular protein targets. This modification is catalysed by the enzymatic actions of the mono-ADP-ribosyltransferases (mARTs), and can be reversed by ADP-ribosyl hydrolases, which cleave this covalent bond to release the target protein [12–15].

In mammals, two groups of mARTs have been identified and classified: the ARTDs (diphtheria toxin like) and the ARTCs (clostridia toxin like) [16]. Recently, we and others have demonstrated that some members of the ARTD family are active mARTs [17, 18]. In contrast to the mARTs of the ARTD family, those of the ARTC family have been known for longer. The ARTC family is relatively small and includes four human subtypes (hARTC1, 3, 4, 5) and six murine subtypes (ARTC1, 2.1, 2.2, 3, 4, 5) that are glycosylphosphatidylinositol (GPI)-anchored or secreted proteins [19]. ARTC1, 2 and 5 have been characterised as arginine-specific mARTs. The catalytic domain of the ARTCs is coded by a single exon that is present in all of these ARTCs, and it contains an arginine-serine-glutamate (R-S-E) triad of amino-acid residues, where the glutamate residue is conserved, and is crucial for the catalytic activity. The motif R-S-EXE is typical of these arginine-specific ARTs, although it is missing in ARTC3 and ARTC4, which may be inactive as enzymes [19]. The arginine-specific ARTC1, 2, and 5 have been reported to modify soluble and plasma-membrane-associated protein targets on arginine residues, including the $P2X_7$ purinergic receptor, human neutrophil protein 1, and α7 integrin [20–22], and thus they can affect cellular processes such as intercellular signalling, immune responses, and inflammation [13, 19, 23, 24]. We recently cloned a hamster orthologue of ARTC2 from CHO cells, which we named cARTC2.1, and we have shown that it is an arginine-specific ARTC that is characterised by the R-S-EKE motif. We have also shown that the double mutation of Glu-207 and Glu-209 of the cARTC2.1 EKE catalytic sequence leads to its complete loss of activity [25].

In the present study, we extended our search for target proteins that are ADP-ribosylated in cells overexpressing the ARTCs, and we demonstrate that the endoplasmic reticulum (ER) luminal chaperone GRP78 (glucose-regulated protein of 78 kDa) is a cellular target for cARTC2.1, and more importantly, for hARTC1.

GRP78 is also known as BiP (immunoglobulin heavy chain-binding protein), and it was initially described in 1977 [26]. It is a luminal ER molecular chaperone that is ubiquitously expressed in mammalian cells [27–29]. GRP78/BiP is a member of the 70-kDa heat-shock protein (HSP70) family that is characterised by a conserved ATPase domain and a peptide-binding domain, and it has a central role in ER-mediated cellular processes [30]. GRP78/BiP associates transiently with nascent peptides, facilitates their co-translational translocation from the ribosome to the ER, and mediates the folding and transport of the newly synthesised proteins through the ER, to prevent non-specific aggregation of misfolded or unfolded proteins. Moreover, GRP78/BiP targets misfolded proteins for ER-associated protein degradation [31–33]. Thus, as well as its role in the folding and assembly of proteins, GRP78/BiP can trigger the unfolded protein response (UPR) [34]. Indeed, when protein production exceeds a certain threshold, or when unfolded proteins are generated, GRP78/BiP dissociates from its interactors, which include PERK (double-stranded RNA-dependent protein kinase (PKR)-like ER kinase), ATF6 (activating transcription factor 6) and IRE1α (inositol-requiring 1α); this then leads to the activation of ER stress responses [35, 36]. These three GRP78/BiP interactors are transmembrane proteins that have an ER-lumen domain that can sense unfolded proteins, a transmembrane domain through which they can associate with the ER membrane, and a cytosolic domain that transmits signals to the transcriptional or translational apparatus. In resting cells, all three of these ER-stress sensors are maintained in an inactive state through their association with GRP78/BiP [35, 36]. Among the chemical activators of the UPR, dithiothreitol (DTT) and thapsigargin are known to cause acute inhibition of the synthesis of all cellular proteins (which occurs with 10–20 min of treatment), with the exception of GRP78/BiP [37]. The subsequent recovery of protein synthesis and induction of

GRP78/BiP require a minimum of 2 h, and plateau within 12–18 h, depending on the cell type (reviewed in [37]). The increased levels of GRP78/BiP and of other chaperones enhance the ER protein folding capability. Thus, GRP78/BiP is a central mediator of both acute inhibition of translation initiation and its subsequent recovery.

It was previously shown that mono-ADP-ribosylation of GRP78/BiP can regulate the availability of functional GRP78/BiP; indeed, this post-translational modification has been detected in response to nutritional stress, and it appears to provide a buffering system that allows the rates of protein processing to be balanced with those of protein synthesis [38–40]. More recently, it has been shown that mono-ADP-ribosylation of GRP78/BiP occurs on two arginine residues (R470, R492) in the substrate-binding domain of GRP78/BiP, and analysis of the mutated protein is in line with the concept that this post-translational modification can interfere with substrate binding [41].

We previously postulated that an arginine-specific enzyme of the ARTC family would be needed to modify GRP78 [13]. *Macro*-domains can interact with monomeric, polymeric, or both forms of ADP-ribose, or with other NAD derivatives [42–44]; thus based on our recent discovery that the '*macro* domain' Af1521 (*m*Af1521) can be used as selective bait for high-affinity purification of ADP-ribosylated proteins [42], we demonstrate here that human ARTC1 ADP-ribosylates GRP78, suggesting that this post-translational modification represents the cellular strategy for the rapid regulation of the activity of this important ER chaperone.

Materials and methods

Cell culture and fractionation

Human cervix adenocarcinoma (HeLa) cells (European Collection of Cell Cultures, UK) were grown in Eagle's minimal essential medium (Lonza, Basel, Switzerland) supplemented with 100 U penicillin, 100 µg/ml streptomycin, 1 % minimal essential medium non-essential amino acids, 10 % foetal calf serum, and 4 mM L-glutamine (Life Technologies, Monza, Italy). Chinese hamster ovary (CHO) cells were grown as previously described, in Dulbecco's modified Eagle's medium (Lonza, Basel, Switzerland) supplemented with 100 U penicillin, 100 µg/ml streptomycin, and 10 % foetal calf serum (Life Technologies, Monza, Italy) [45]. Human embryonal kidney (HEK293T) cells were grown in Dulbecco's modified Eagle's medium supplemented with 2 mM L-Glutamine, 1 mM Sodiumpyruvate, 10 mM HEPES and non-essential aminoacids, and 5 % foetal calf serum. The cells were grown under a controlled atmosphere in the presence of 5 % CO_2 at 37 °C. Total membranes and post-nuclear fractions were prepared as previously described [42, 46]. Cell lysates were prepared as previously described [47]. Protein concentrations were determined with the Bio-Rad protein assay (Bio-Rad).

Plasmids, transfection and silencing

The plasmids for the cDNAs for CD8-Flag-hARTC1, CD8-Flag-hARTC4, CD8-Flag-cARTC2.1, CD8-Flag-cART C2.1-E207G/E209G, and Flag-hARTC1-E238G/E240G were produced as previously described [25, 48]. CHO cells were transfected using Lipofectamine reagent, as instructed by the supplier (Invitrogen Corporation, Carlsbad, CA, USA). HeLa and HEK293T cells were transfected using the jetPEI transfection reagent (Polyplus-Transfection SA, Illkirch, France). To silence hARTC1, HeLa cells were transfected with a pool of three siRNAs (30 nM), using jetPRIME (Polyplus). The following siRNAs (Sigma) were used: 1) AUGCAUGAGACACGGGACA; 2) ACACGGA GUUCCAGGCCAA; 3) GCGAGUACAUCAAAGACAA. Here, 70 % of endogenous hARTC1 was knocked-down after 48 h (as evaluated by Quantitative real-time (qRT)-PCR). To silence GRP78, HeLa cells were transfected with siGENOME Human HSPA5 siRNA reagents (100 nM; Thermo Scientific Dharmacon), using jetPRIME (Polyplus). As control, the following scrambled oligonucleotides (Sigma) were used: (1) GGUAAUCAACUAAUCUUAA; (2) UUAAGAUUAGUUGAUUACC.

Immunoprecipitation and ADP-ribosylation assay

HEK293T cells were either untransfected (control), or transfected with Flag-GRP78 or co-transfected with Flag-GRP78 and Flag-hARTC1 [49]. After 24 h, the cells were lysed in Dulbecco's phosphate-buffered saline containing 1 % Triton X-100, 1 mM ADP-ribose, 1 mM AEBSF, and 0.1 U PI-PLC (Life-Technologies) for 20 min at 37 °C. The lysates were cleared by centrifugation (16.000×*g* for 10 min at 4 °C) and subjected to immunoprecipitation with an agarose immobilised anti-Flag monoclonal antibody (M2-Affinity Gel, Sigma) for 1 h at 4 °C (106 cells/20 µl). The resins was centrifuged and washed four times with Dulbecco's phosphate-buffered saline containing 1 % Triton X-100. The bound proteins were eluted with 100 mM glycine, pH 2.7 (20 µl). The pH of the eluted protein solution was neutralised by addition of 1 M Tris, pH 9 (2 µl). The eluted proteins were incubated with [^{32}P]-NAD^{+} for 15 min at 37 °C and then separated by SDS-PAGE. Radiolabelled proteins were detected using autoradiography, by exposure of an X-ray film (Hyperfilm, GE-Healthcare) for 3 h at −80 °C.

Western and far-Western blotting

Cell lysate were prepared as described in [41]. Cell lysate proteins (70 µg) were separated by 8 % SDS-PAGE (unless otherwise indicated) and transferred to nitrocellulose filters (Perkin Elmer). For Western blotting, the filters were incubated with the primary antibodies diluted in T-TBS for 1 h at room temperature, or overnight at 4 °C. The following primary antibodies were used: rabbit and mouse anti-Flag, rabbit anti-actin, mouse anti-tubulin, and rabbit anti-ARTC1 from Sigma-Aldrich; mouse anti-GRP78 (BD Bioscience); and mouse anti-GAPDH (Santa Cruz). Western blotting with the anti-ARTC1 antibody revealed at least four major bands that would reflect different degrees of glycosylation of hARTC1. For far-Western blotting, the filters were first incubated with 20 ng/ml glutatione S-transferase (GST)-tagged *m*Af1521 in binding buffer (50 mM Tris–HCl, pH 7.4, 100 mM NaCl, 1.5 mM $MgCl_2$, 0.5 mM DTT, 10 % foetal bovine serum) for 1 h at room temperature. The filters were then washed and incubated with a polyclonal, rabbit anti-GST antibody (generated by us against human GST and affinity-purified using GST as immunogen) for 3 h at room temperature. After washes with T-TBS, the filters were incubated with horseradish-peroxidase-conjugated anti-mouse or anti-rabbit antibodies (Calbiochem). Protein bands were visualised with the ECL western blotting detection reagents (GE-Healthcare), according to manufacturer's instructions. Densitometric evaluation was carried out with the public domain ImageJ software.

Macro-GST pull-down assay

The *macro*-domain-based pull-down assay and protein identification by matrix-assisted laser desorption/ionisation time-of-flight mass spectrometry (MALDI-TOF–MS) were performed as previously described, using the GST-tagged *m*Af1521 (wild type) and *m*Af1521-G42E (which does not bind ADP-ribosylated proteins) *macro* modules [45]. Briefly, total cell lysates (3 mg per sample) were solubilised in RIPA buffer (100 mM Tris/HCl, pH 7.5, 1 % Igepal, 0.5 % deoxycholate, 0.1 % SDS, protease inhibitors) with constant rotation for 30 min at 4 °C. The mixture was briefly sonicated on ice and clarified by centrifugation at 16,000×*g* for 45 min at 4 °C. The supernatant was incubated with GST resin that had been previously cross-linked with the *m*Af1521-G42E. The supernatant underwent sequential pull-down with GST resin cross-linked with the *m*Af1521. Then the resin was washed five times with RIPA buffer, and finally both the washed resins were diluted in 100 µl of Laemmli buffer, boiled and analysed by 12 % SDS-PAGE. The gels underwent colloidal Coomassie blue staining (blue code, Pierce), and the bands of interest were analysed by MALDI-TOF–MS, as described previously [32].

Immunofluorescence and confocal microscopy

Cells were grown on coverslips in 24-well plates and transfected either with Lipofectamine-Plus (Invitrogen) or with the jetPEI transfection reagent (Polyplus-Transfection SA, Illkirch, France). After 24 h, the cells were washed with phosphate-buffered saline (PBS), fixed in 4 % paraformaldehyde (in PBS) for 10 min, and then permeabilised in blocking solution (0.05 % saponin, 0.5 % bovine serum albumin, 50 mM NH_4Cl, in PBS). The overexpressed ARTC proteins were detected with a mouse anti-Flag antibody (M2-Sigma; 1:500 in blocking solution); and GRP78 was stained with a rabbit anti-GRP78 antibody (Santa Cruz; 1:100 in blocking solution). The endogenous protein disulfide isomerase (PDI) protein was detected with an anti-PDI antibody (Stressgen; 1:200 in blocking solution); the endogenous hARTC1 was stained with a rabbit anti-ART1 antibody (AbCam; 1:70 in blocking solution); the endogenous protein calnexin was detected with a mouse anti-Calnexin antibody (BD Transduction Laboratories; 1:50 in blocking solution). The cells were washed twice with PBS then once briefly with water. The cover slips were mounted on glass slides with Mowiol 4-88 and dried at 4° C overnight. The samples were analysed under a confocal microscope (Zeiss LSM 510; Zeiss, Thornwood, NY, USA). The co-localization analysis of ARTC enzymes with PDI or with other proteins in the cells was performed with LSM510-3.2 software (Zeiss). To assess the co-localization we removed the background immunofluorescence by adjusting the threshold levels and used the histo and co-localization functions of the above software. This software provides two co-localization coefficients that range from 0 (no co-localization) to 1 (complete co-localization). The co-localization coefficients indicate the amount of pixels of the channel A that co-localises with pixels from channel B and viceversa. Finally, we expressed the co-localization extent as a percentage over the total immunofluorescence per channel.

GST-*m*Af1521 immunofluorescence staining

The *macro*-domain-based immunofluorescence was performed as described in the previous section, with the difference that the cells were fixed, permeabilised and then incubated for 1 h with *m*Af1521 or *m*Af1521-G42E (6 ng/µl in blocking solution). The cells were washed with PBS, and the ADP-ribosylated proteins were detected with the rabbit anti-GST antibody (1:1,000 in blocking solution).

Table 1 List of primers used in this study

Primer name	Primer sequence
ARTC1qRT For	GGCCTCATGGAAGCACTTCA
ARTC1qRT Rev	GAGAAGAGGTCTCGTCGTGTGA
GRP78/BiPqRT For	ACGTGGAATGACCCGTCTGT
GRP78/BiPqRT Rev	AACCACCTTGAACGGCAAGA
GAPDHqRT For	CAACTTTGGTATCGTGGAAGGAC
GAPDHqRT Rev	ACAGTCTTCTGGGTGGCAGTG

Quantitative real-time PCR

Quantitative real-time (qRT)-PCR was performed as described previously [25]. The primer sequences for the human ARTC1, GRP78 and glyceraldeyde-3-phosphate dehydrogenase (GAPDH) genes (Table 1) were designed using the Primer Express 3.0 software (Applied Biosystems). The quantitative normalisation of the cDNA in each sample was carried out using GAPDH (accession number: X52123.1) amplification as the internal control. The relative quantification was determined using the comparative ΔΔCT method.

Statistical analysis

Data are expressed as mean ± standard deviation. Unpaired Student's *t* tests were performed on the means, and the *p* values were calculated using GraphPad PRISM software version 4.0b. A $p < 0.05$ was considered statistically significant, unless otherwise indicated. For the co-localization analysis, values are expressed as mean ± standard error of the mean (SEM) and analysed by one-way analysis of variance (ANOVA), calculated using GraphPad PRISM software version 4.0b. A $p < 0.05$ was considered significant unless otherwise indicated.

Results

cARTC2.1 and hARTC1 mediate ADP-ribosylation of GRP78

We recently cloned and characterised a GPI-anchored, arginine-specific, mART from CHO cells, which we named cARTC2.1 [25]. In the present study, we extended our search for target proteins that are ADP-ribosylated by cARTC2.1, taking advantage of our previous demonstration that the *m*Af1521 specifically recognises and binds ADP-ribosylated proteins, which can then be identified by mass spectrometry [42].

To this end, we initially analysed CHO cells transfected with Flag-cARTC2.1 (as the wild-type) or with its inactive double mutant Flag-cARTC2.1-E207G/E209G (Fig. 1a). The cell lysates were subjected to two-step pull-down with the GST-tagged *macro* domains: the first pull-down was performed using the GST-tagged *m*Af1521/G42E mutant, which does not bind ADP-ribosylated proteins [42]. Then, the unbound material underwent a second pull-down with wild-type GST-*m*Af1521, to specifically retain ADP-ribosylated proteins. The pulled-down proteins obtained following this two-step procedure were separated by 10 % SDS-PAGE and revealed by colloidal Coomassie blue staining. A significant band of ca. 78 kDa was detected in the Flag-cARTC2.1 transfected CHO cells and was identified by MALDI-TOF–MS analysis as the highly conserved ER chaperone protein GRP78/BiP (referred to here now as GRP78; Fig. 1a). No band corresponding to GRP78 was detected when the same pull-down assay was performed with cells transfected with the inactive cARTC2.1-E207G/E209G (Fig. 1a, dm). Thus, GRP78 can be ADP-ribosylated by cARTC2.1. We next investigated whether hARTC1, the closest functional human homologue of ARTC2.1, can induce GRP78 ADP-ribosylation. To this end, CHO cells transfected with Flag-hARTC1 were analysed by the two-step pull-down assay (Fig. 1b). Although to a lower extent compared with cARTC2.1, GRP78 was also pulled-down from cells transfected with Flag-hARTC1 (Fig. 1b), while it was not pulled-down from cells transfected with the empty vector alone (pME.CD8LF; Fig. 1b, control) or with the inactive hARTC4 (data not shown).

These findings indicate that catalytically active cARTC2.1 and hARTC1 can specifically induce ADP-ribosylation of GRP78, suggesting that these arginine-specific mARTs are involved in the previously described intracellular GRP78 mono-ADP-ribosylation [42].

Use of the *macro* module to visualise ADP-ribosylated proteins by immunofluorescence microscopy

The finding that the *m*Af1521 specifically pulled down GRP78 in cells transfected with hARTC1 and cARTC2.1 prompted us to investigate whether the *m*Af1521 can be used to visualise ADP-ribosylated proteins by immunofluorescence.

Here, we first set up the conditions for immunofluorescence using the GST-tagged wild-type and mutant *m*Af1521 (see Methods, Fig. 2). We detected ADP-ribosylated proteins in cells that had been previously fixed and permeabilised and then incubated with the *macro* domain. Under these experimental conditions, the *macro* domain bound to ADP-ribosylated proteins that were then detected using an anti-GST antibody. HeLa cells were initially transfected with the empty vector (pME.CD8LF; Fig. 2a, b, controls) and analysed by immunofluorescence. The staining with GST-*m*Af1521 (wild-type) was mainly

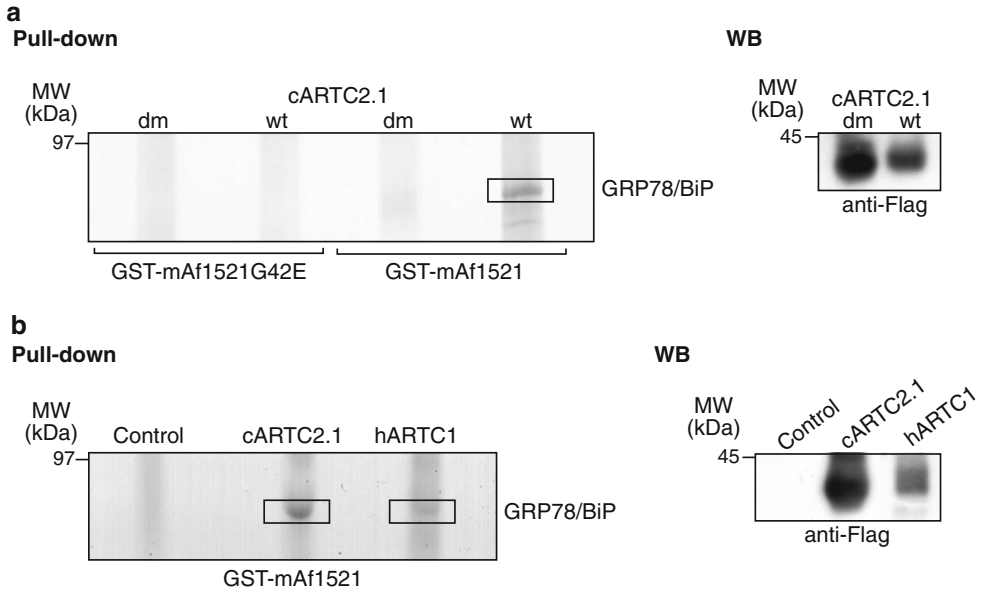

Fig. 1 *Macro*-domain-based pull-down assay coupled to MALDI-TOF–MS analysis identifies GRP78 as a substrate of the ARTCs. **a**, **b** Representative pull-down from CHO cells transfected with hARTC1 and cARTC2.1. wt, enzymatically active wild type; dm, enzymatically inactive double mutant. Cell lysates (3 mg protein) underwent non-specific pull-down step using the GST-tagged *m*Af1521/G42E mutant (with abrogated binding of *m*Af1521 ADP-ribosylated proteins [32]). Unbound material underwent a second pull-down with wild-type GST-*m*Af1521, to specifically retain ADP-ribosylated proteins. This two-step procedure resulted in separation of specific proteins that were revealed by colloidal Coomassie blue staining and identified by MALDI-TOF analysis (NCBI acc. Number: AAA52614; Score: 209; Matched peptide no.: 21; Sequence coverage: 35 %; Molecular mass: 72 kDa; Protein scores ≈ 65 are significant ($p < 0.05$). Western blotting (WB) shows the levels of expression of the indicated Flag-tagged proteins, as performed by immunoblotting with an anti-Flag antibody. The data shown are representative of at least five independent experiments

nuclear (Fig. 2a), which suggested that in these cells under basal condition, nuclear ADP-ribosylation can be detected. The specificity of this labelling was confirmed by the lack of cell staining when the GST-tagged *m*Af1521/G42E (mutant) was used (Fig. 2b). Moreover, there was no detectable Flag staining in mock-transfected cells. Thus, this represented a very efficient method to visualise ADP-ribosylated proteins by immunofluorescence.

HeLa cells were then transfected with Flag-hARTC1 (wild-type; Fig. 2c, d), Flag-hARTC4 (inactive control; Fig. 2e, f), Flag-cARTC2.1 (wild-type; Fig. 2g, h), or the cARTC2.1 double mutant Flag-cARTC2.1-E207G/E209G (inactive control; Fig. 2i, j, cARTC2.1-dm). They were then analysed by immunofluorescence microscopy with an anti-Flag antibody to detect the overexpressed enzymes, and with the GST-tagged *m*Af1521 and anti-GST antibody to visualise ADP-ribosylation. The immunofluorescence images showed clear peri-nuclear staining of hARTC1 (Fig. 2c, d). Minimal peri-nuclear staining was seen for hARTC4 (Fig. 2e, f). The staining of cARTC2.1 (Fig. 2g, h) and its double mutant (Fig. 2i, j) showed that they were correctly localised to the cell periphery, as previously reported [25]. Of note, GST-*m*Af1521 revealed a peri-nuclear staining in cells transfected with enzymatically active hARTC1 (Fig. 2c) or with enzymatically active cARTC2.1 (Fig. 2g), in line with ADP-ribosylation events occurring at the ER level. In contrast, cells transfected with the inactive proteins, hARTC4 and cARTC2.1-E207G/E209G, showed nuclear staining with GST-*m*Af1521 (Fig. 2e, i, respectively), as in control cells (Fig. 2a). Finally, the mutated GST-*m*Af1521/G42E that cannot bind ADP-ribosylated proteins showed no staining in transfected cells (Fig. 2d, f, h, j), as expected. As a further control, HeLa cells were transfected with a hARTC1 double mutant, as the catalytically inactive Flag-hARTC1-E238G/E240G. The immunofluorescence images show nuclear staining with GST-mAf1521 (Supplementary Fig. S1A), as in the control and in Flag-hARTC4-transfected cells.

These data provide a technological advance in the study of ADP-ribosylation by immunofluorescence microscopy. A prominent GST-*m*Af1521-dependent perinuclear staining of cells was seen upon transfection with the active enzymes hARTC1 and cARTC2.1, but not with their inactive counterparts. Thus, GST-*m*Af1521 perinuclear staining correlates with hARTC1-mediated and cARTC2.1-mediated GRP78 ADP-ribosylation occurring using endogenous NAD^+ within the lumen of the ER, where GRP78 is known to reside.

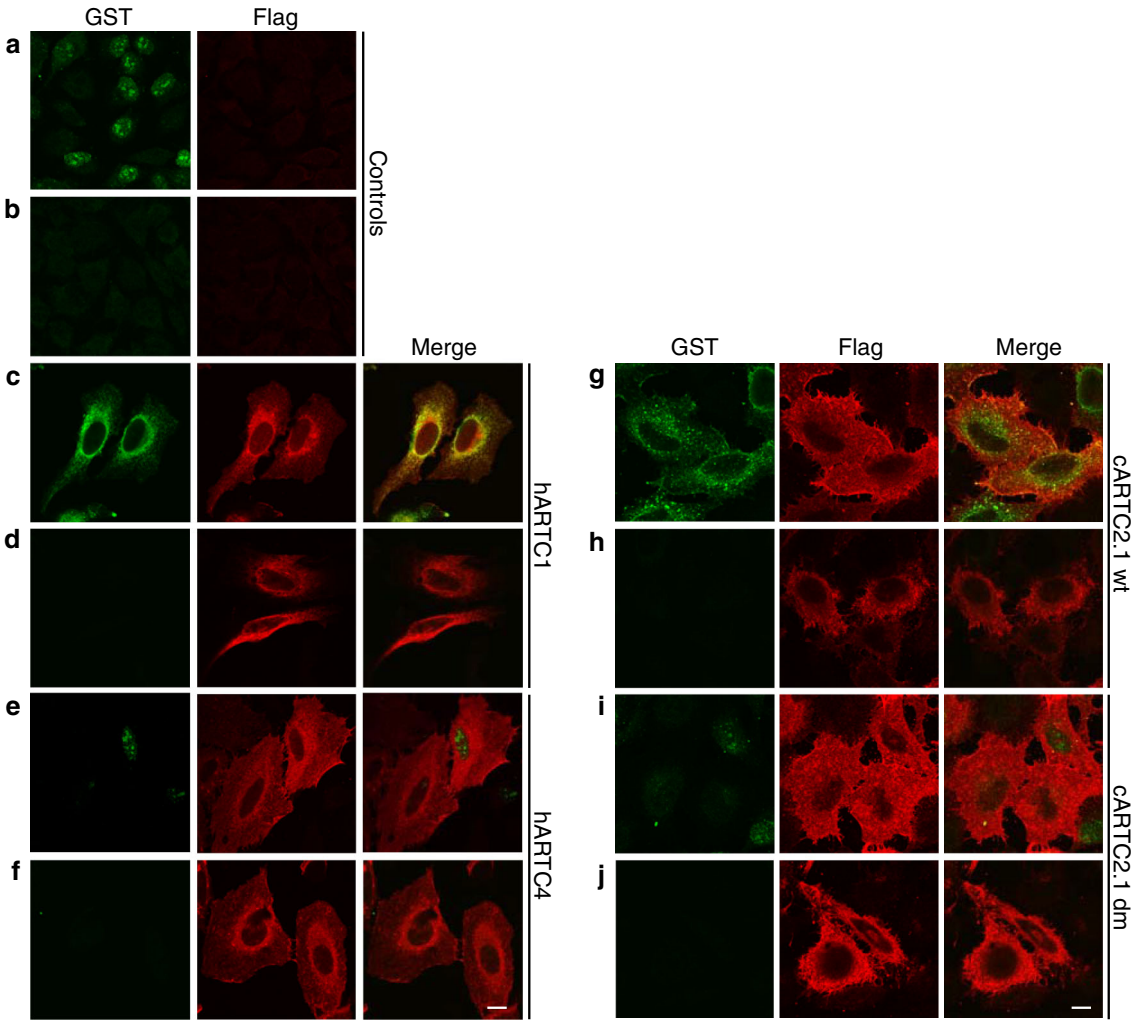

Fig. 2 The *m*Af1521 *macro* module can be used to visualise ADP-ribosylated proteins. Representative immunofluorescence images of HeLa cells that were left non-transfected (controls; **a**, **b**) or were transiently transfected with the indicated constructs (**c**–**j**) and incubated with GST-*m*Af1521 (**a**, **c**, **e**, **g**, **i**) or GST-*m*Af1521/G42E (**b**, **d**, **f**, **h**, **j**), and stained with anti-Flag and anti-GST antibodies, as indicated, and analysed by immunofluorescence. *Bar* 10 µm. The data shown are representative of at least ten independent experiments

hARTC1 localises to the ER and co-localises with GRP78

To further investigate whether the perinuclear staining revealed by immunofluorescence with GST-*m*Af1521 in cells overexpressing hARTC1 and cARTC2.1 was due to ADP-ribosylated GRP78, HeLa cells were transfected with Flag-hARTC1, Flag-hARTC4, Flag-cARTC2.1, and Flag-cARTC2.1-E207G/E209G, as indicated (Figs. 3, 4), and then analysed by immunofluorescence microscopy with an anti-GRP78 antibody in combination with either GST-*m*Af1521 and an anti-GST antibody (Fig. 3), or an anti-Flag antibody (Fig. 4).

Immunofluorescence images of cells overexpressing hARTC1 and cARTC2.1 showed that the staining with GST-*m*Af1521 co-localised with GRP78 staining (Fig. 3a, e). As expected, there was no co-localisation between GRP78 and GST-*m*Af1521 when the cells were transfected with the inactive proteins hARTC4 or cARTC2.1-E207G/E209G (Fig. 3c, g), consistent with the notion that GRP78 is ADP-ribosylated as a consequence of either hARTC1 or cARTC2.1 overexpression. GST-*m*Af1521/G42E did not stain transfected cells (Fig. 3b, d, f, h), as expected.

The immunofluorescence analysis with the anti-GRP78 and anti-Flag antibodies indicate that hARTC1 resides in the same peri-nuclear area where GRP78 also resides, thus suggesting that these two proteins can co-localise at the ER (Fig. 4a). When overexpressed in HeLa cells, Flag-hARTC1-E238G/E240G shows a similar distribution to the Flag-hARTC1 wild-type protein, as it also co-localises with GRP78 (Fig. S1A). Of note, although cARTC2.1 was physically separated from GRP78 (Fig. 4c), it can induce

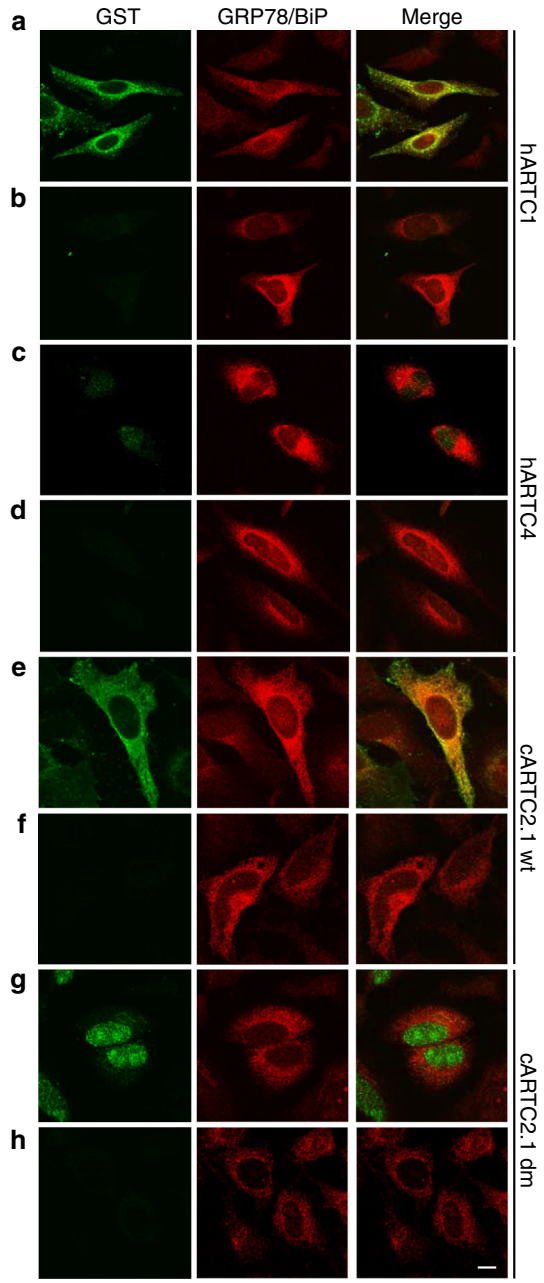

Fig. 3 The *m*Af1521 *macro* module staining co-localises with GRP78. Representative immunofluorescence images of HeLa cells that were transiently transfected with the indicated constructs and incubated with GST-*m*Af1521 (**a**, **c**, **e**, **g**) or GST-*m*Af1521/G42E (**b**, **d**, **f**, **h**), and stained with anti-GST and anti-GRP78 antibodies, as indicated, and analysed by immunofluorescence. *Bar* 10 μm. The data shown are representative of at least five independent experiments

GRP78 ADP-ribosylation (Figs. 1-3), in line with its action as an arginine-specific ART, and noting that as a GPI-anchored protein, it is transiently present into the ER.

Finally, we developed *macro*-domain-based far-Western blotting (see Methods; Fig. 5) to directly visualise

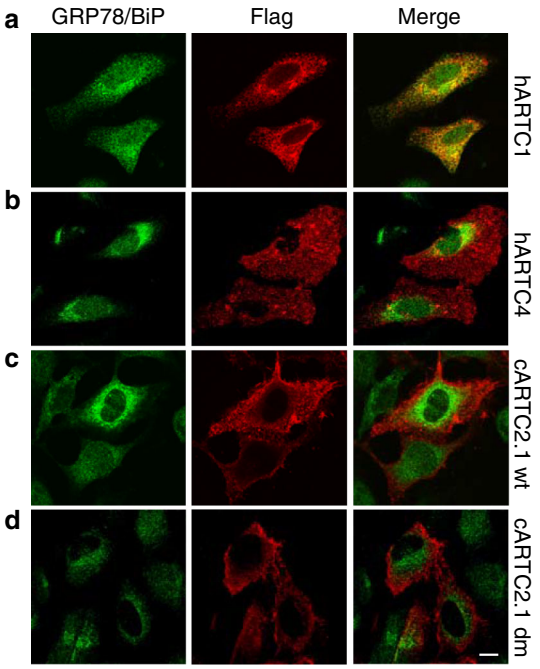

Fig. 4 hARTC1 co-localises with GRP78. Representative immunofluorescence images of HeLa cells that were transiently transfected with the indicated constructs and stained anti-GRP78 or anti-Flag antibodies, as indicated, and analysed by imunofluorescence. *Bar* 10 μm. The data shown are representative of at least five independent experiments

Fig. 5 GRP78 can be ADP-ribosylated by the ARTCs. **a** Representative far-Western blotting (FAR-WB) with GST-tagged *m*Af1521 for HeLa cells transfected with the empty vector (control) or with the indicated constructs. The solubilised proteins were separated by SDS-PAGE, transferred to nitrocellulose filters, and incubated with GST-tagged *m*Af1521 (see "Methods"). Representative Western blotting (*WB*, *bottom*) showing that the indicated band in (**a**, *top*) was recognised by a specific anti-GRP78 antibody. The levels of expression of the indicated Flag-tagged proteins and the actin loading control are also shown. The data shown are representative of at least three independent experiments. **b** Cell lysates from HEK293 cells transfected with empty vector (control) or Flag-GRP78/BiP, or co-transfected with Flag-GRP78/BiP and Flag-hARTC1 were immunoprecipitated with the Sepharose-immobilised M2 anti-Flag antibody. The eluted proteins were incubated with [32P]-NAD (15 min), then separated by SDS-PAGE, and analysed by autoradiography (AR) and by Coomassie staining. **c**, **d** Representative far-Western blotting (FAR-WB) with GST-tagged *m*Af1521 of both control (scrambled) and hARTC1-silenced (**c**) or GRP78/BiP-silenced HeLa cells (**d**). The solubilised proteins were separated by SDS-PAGE, transferred to nitrocellulose filters, and incubated with GST-tagged *m*Af1521 (see "Methods"). The Western blotting (WB) shows the hARTC1 (**c**) or GRP78/BiP knock-down (**d**). Western blotting with the anti-ARTC1 antibody revealed at least four major bands that would reflect different degrees of glycosylation of hARTC1. The Western blotting also shows the levels of expression of GRP78, and of GAPDH (**c**) and tubulin (**d**). The data shown are representative of at least three independent experiments. *Asterisk* significantly different from the relevant control ($p < 0.05$)

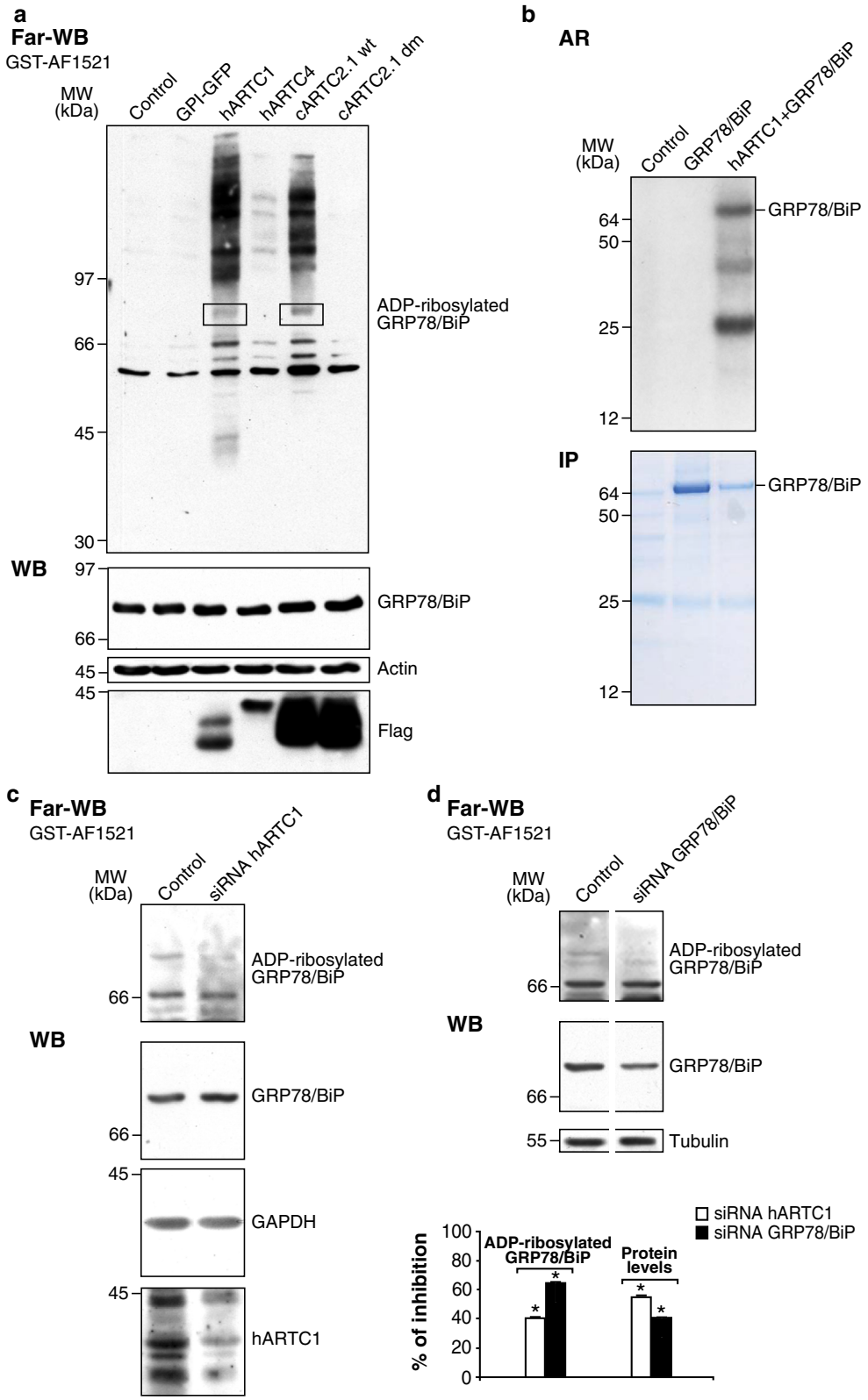
a
Far-WB
GST-AF1521
MW (kDa)
Control
GPI-GFP
hARTC1
hARTC4
cARTC2.1 wt
cARTC2.1 dm
97
66
45
30
ADP-ribosylated GRP78/BiP
WB
97
66
GRP78/BiP
45
Actin
45
Flag
b
AR
MW (kDa)
Control
GRP78/BiP
hARTC1+GRP78/BiP
64
50
25
12
GRP78/BiP
IP
64
50
25
12
GRP78/BiP
c
Far-WB
GST-AF1521
MW (kDa)
Control
siRNA hARTC1
66
ADP-ribosylated GRP78/BiP
WB
66
GRP78/BiP
45
GAPDH
45
hARTC1
d
Far-WB
GST-AF1521
MW (kDa)
Control
siRNA GRP78/BiP
66
ADP-ribosylated GRP78/BiP
WB
66
GRP78/BiP
55
Tubulin
siRNA hARTC1
siRNA GRP78/BiP
% of inhibition
100
80
60
40
20
0
ADP-ribosylated GRP78/BiP
Protein levels
*

ADP-ribosylated GRP78. Cell lysates from HeLa cells previously transfected with the empty vector (pME.CD8LF; control), a GFP-GPI construct, or Flag-tagged hARTC1, hARTC4, cARTC2.1, and cARTC2.1-E207G/E209G (Fig. 5a, as indicated) were separated by SDS-PAGE, and the proteins transferred to nitrocellulose filters that were then incubated with GST-*m*Af1521. Numerous protein bands, including a protein band with the predicted molecular weight of GRP78 were visualised with the anti-GST antibody (Fig. 5a, Far-WB) only in cells transfected with the enzymatically active ARTs, cARTC2.1 and hARTC1. A band at the same height was recognised by an anti-GRP78 antibody (Fig. 5a, WB). No band was visualised with the anti-GST antibody in far-WB when HeLa cells were transfected with the inactive Flag-hARTC1-E238G/E240G (Fig. S1B). When the filters were incubated with GST-*m*Af1521/G42E no signal was detected at all (data not shown).

In order to directly assess whether hARTC1 can ADP-ribosylate GRP78, we performed a [^{32}P]-ADP-ribosylation assay using purified proteins and exogenously added [^{32}P]-NAD^{+}. To this end, HEK293T cells were co-transfected with Flag-GRP78 and Flag-hARTC1. For controls, cells were not transfected or transiently transfected with Flag-GRP78 alone. The Flag-tagged proteins in lysates from these cells were immunoprecipitated with the M2 anti-FLAG antibody, and the eluted proteins were then incubated with [^{32}P]-NAD^{+} and analysed by autoradiography (Fig. 5b, AR). Three bands were revealed in Flag-GRP78 and Flag-hARTC1 co-transfected sample: a lower band with a molecular mass of ca. 25, which corresponds to the light chain of the M2 antibody, an intermediate band of ca. 38 kDa that corresponds to hARTC1, and a higher band of ca. 78 kDa that corresponds to GRP78. These results show that ARTC1 might, indeed, ADP-ribosylate GRP78.

Furthermore, when lysates of untransfected HeLa cells were subjected to far-Western blotting with GST-tagged wild-type *m*Afl521, a distinct band corresponding in size to GRP78 could be detected in longer exposures (Fig. 5c, d). This staining of this band was reduced by approximately 40 and 65 % when endogenous hARTC1 (Fig. 5c) or GRP78 (Fig. 5d), respectively, were knocked-down by siRNA.

These results support the notion that hARTC1 is the endogenous enzyme responsible for the ADP-ribosylation of GRP78.

ARTC1 is an ER-resident protein

Immunofluorescence microscopy of ARTC1-transfected cells suggested that hARTC1 is preferentially located in the ER (Figs. 3, 4). To further investigate the cellular localisation of hARTC1, immunofluorescence was carried out in the presence of cycloheximide, to inhibit new protein synthesis and hence to ensure that no fluorescence was preferentially gained by the ER compartment due to new protein synthesis. Here, HeLa cells expressing hARTC1, hARTC4, cARTC2.1, and cARTC2.1-E207G/E209G (Fig. 6, as indicated) were incubated for 3 h in the absence (Fig. 6, Control) or in the presence (Fig. 6, Chx) of cycloheximide and then analysed by immunofluorescence microscopy.

The ER compartment was stained with an antibody against the endogenous protein disulfide isomerase (PDI), which is one of the most abundant ER-associated proteins. hARTC1 co-localised to a larger extent with PDI in both control and cycloheximide-treated cells (Fig. 6a, c), as opposed to cARTC2.1 and cARTC2.1-E207G/E209G, for which co-localisation with PDI was reduced even further as a consequence of the cycloheximide treatment (Fig. 6b, c). Quantification of these immunofluorescence analyses (Fig. 6c) indicates that 55 % (±4 %) and 6 % (±1 %) of hARTC1 and cARTC2.1, respectively, co-localise with PDI in transfected, non-treated cells. When the cells were treated with cycloheximide, 61 % (±6 %) and 3 % (±0.8 %) of hARTC1 and cARTC2.1, respectively, co-localise with PDI.

Under conditions that block new protein synthesis, as here with cycloheximide, proteins that are not ER-resident will exit the ER compartment, thus reaching their final destination. Our results demonstrate that this is the case for hARTC4, cARTC2.1, and cARTC2.1-E207G/E209G. On the contrary, the treatment with cycloheximide had no effect on the localisation of hARTC1, thus confirming that hARTC1 is located mainly in the ER. Accordingly, the quantification of the immunufluorescence analysis of non-transfected HeLa cells stained with an anti-ARTC1 antibody indicates that 51 ± 2 % of hARTC1 co-localises with the ER protein calnexin (Fig. 6d).

This localisation of hARTC1 was further analysed using additional markers for the ER, Golgi, lysosome and plasma membrane compartments (Supplementary Fig. S2). In addition to its main location at the ER, hARTC1 co-localised with wheat germ agglutinin (WGA; 21 ± 3 %) and to a lower extent with giantin (9 ± 0.8 %) and lamp (7 ± 0.9 %). Quantification of these immunofluorescence analyses (Fig. S2) indicates that only approximately 10 % of ARTC2.1 co-localises with ER proteins, while most of ARTC2.1 co-localises with the plasma membrane (WGA; 53 ± 2 %), as expected.

hARTC1 is an ER stress-sensing protein in mammalian cells

Considering that hARTC1 when located in the ER can induce mono-ADP-ribosylation of GRP78, and considering that GRP78 is a central regulator of ER homeostasis and a

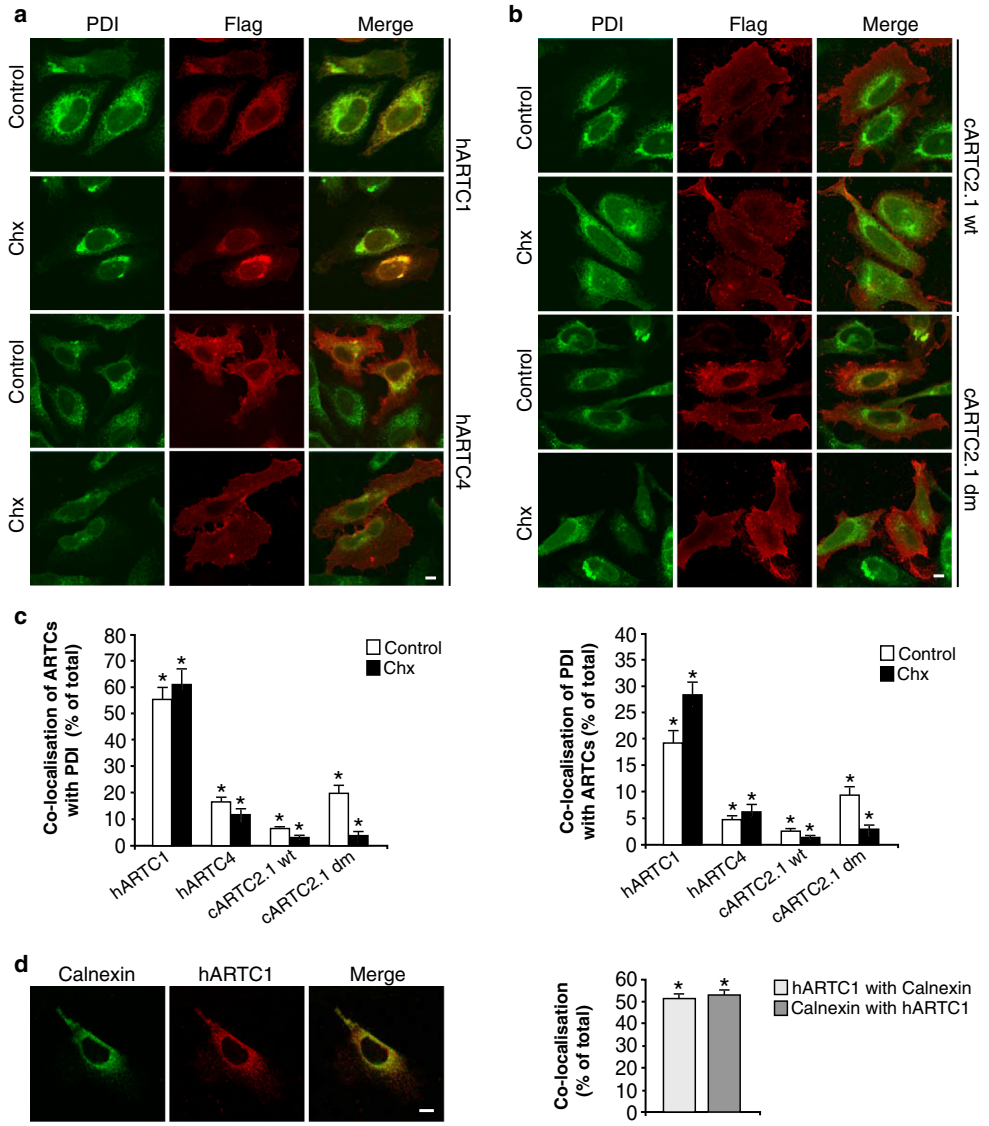

Fig. 6 hARTC1 is located in the ER. **a**, **b** Representative immunofluorescence images of HeLa cells transiently transfected with the indicated constructs and either untreated (control) or incubated with cycloheximide (Chx; 100 µg/ml), stained with anti-Flag or anti-PDI antibodies, as indicated, then analysed by immunofluorescence. *Bar* 10 µm. The data shown are representative of at least three independent experiments. **c** Quantification of at least 50 cells per experiment of three independent experiments is shown in the graph as per cent (mean ± SEM) of the different ARTC enzymes that co-localise with PDI and the per cent of PDI co-localising with the ARTC enzymes. **d** Representative immunofluorescence image of HeLa cells stained with anti-hARTC1 or anti-calnexin antibodies, as indicated. *Bar* 10 µm. The data shown are representative of at least three independent experiments. The quantification of at least 50 cells per experiment of three independent experiments is shown in the *graph* as per cent (mean ± SEM) of hARTC1 that co-localise with calnexin and the per cent of calnexin co-localising with the hARTC1. *Asterisk* significance ($p < 0.0001$)

well-recognised sensor of ER stress, we evaluated whether cell stresses that are known to induce GRP78 can also modulate hARTC1 levels. To this end, we exposed HeLa cells to different stress-inducing treatments, including 2 mM DTT for 2 h, thapsigargin for 2 h, 18 h, and 24 h, heat shock at 42 °C for 24 h, and hypoxia induced by 0.1 % O_2 for 24 h. The mRNA and protein levels of both GRP78 and hARTC1 were determined by quantitative real-time (qRT)-PCR or by Western blotting using antibodies against GRP78 and hARTC1, respectively (Fig. 7).

Compared to control cells, there was strong induction of hARTC1 mRNA (Fig. 7a, left) and protein (Fig. 7b, c: left) levels as a consequence of the DTT and thapsigargin treatments, both of which are well-characterised treatments for the induction of ER stress and GRP78 expression. In line with a well-characterised situation in the field [38], the

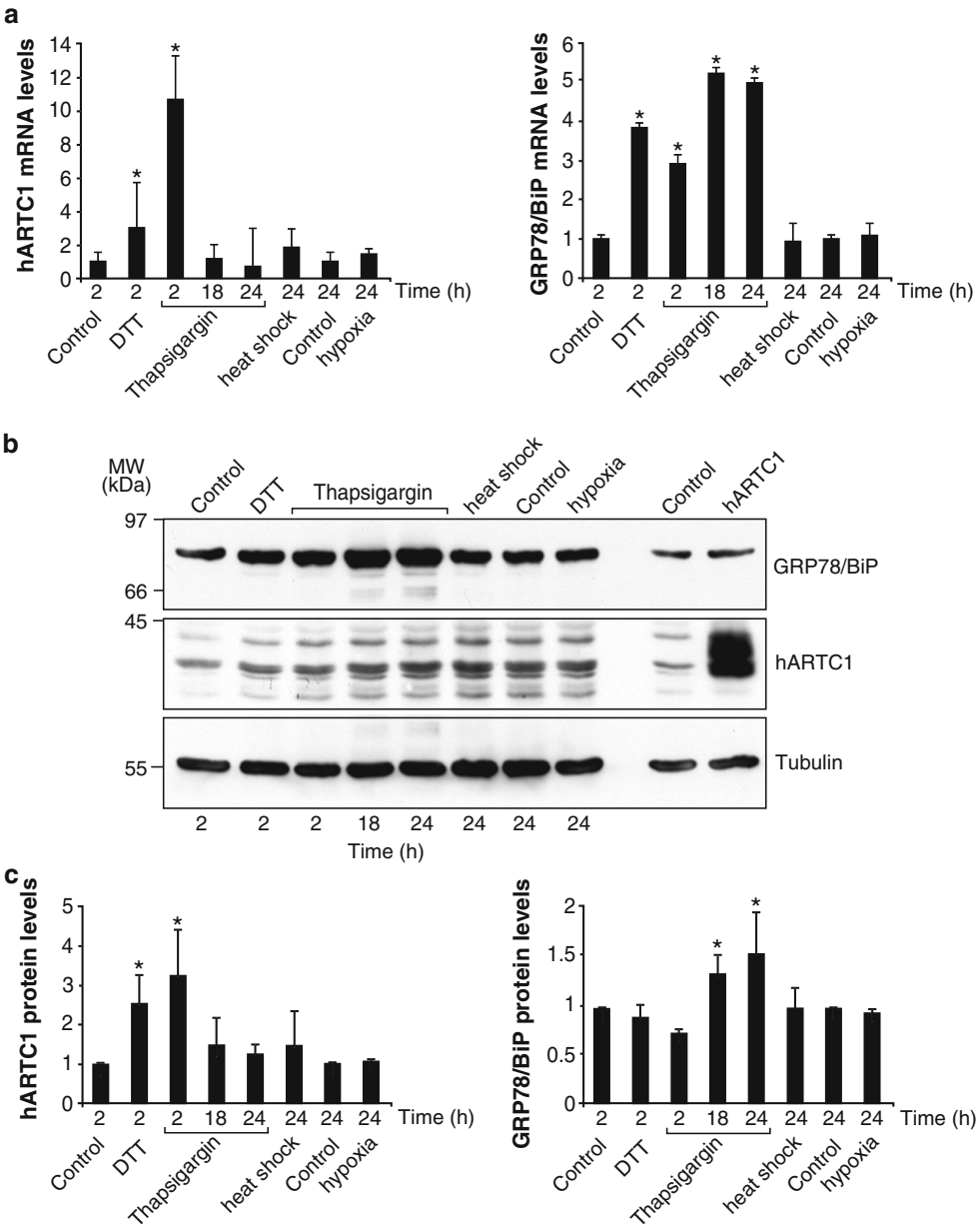

Fig. 7 hARTC1 and GRP78 RNA and protein levels are induced by the cell stressors DTT and thapsigargin. **a** Quantification of the levels of endogenous ARTC1 and GRP78 transcripts determined by qRT-PCR, normalised to GAPDH RNA, and then reported as arbitrary units relative to the ARTC1 or GRP78 transcript in HeLa cells (taken as 1.0). Data are means (±SD) of three independent experiments, each performed in triplicate. *Asterisk* significantly different from the relevant control ($p < 0.01$). **b** Representative Western blotting showing endogenous ARTC1, GRP78, and tubulin levels in 70 μg protein from total cell lysates. **c** Quantification of the protein levels of ARTC1 and GRP78, normalised to tubulin, and relative to those of non-treated cells (control, taken as 1.0). Data are means (±SD) of three independent experiments, each performed in duplicate. *Asterisk* significantly different from the relevant control ($p < 0.05$)

higher GRP78 mRNA levels were observed in HeLa cells treated for 18 h with thapsigargin and were maintained through to 24 h (Fig. 7a, right). Of note here, the greater increase in hARTC1 mRNA was observed after 2 h of 0.3 μM thapsigargin treatment, while levels similar to untreated cells were measured after 18–24 h of 0.3 μM thapsigargin treatment (Fig. 7a, left; also as when 1 μM thapsigargin was used). There were little or no changes in hARTC1 and GRP78 mRNA levels for the other stress treatments (heat shock, hypoxia).

The evaluation of the GRP78 and hARTC1 protein levels under these same incubation conditions (Fig. 7b, c) confirmed that there were increased levels of both GRP78 and hARTC1 as a consequence of the DTT and thapsigargin treatments and confirmed faster kinetics upon ER stress of hARTC1 induction with respect to GRP78. Thus, during the longer term exposure that is suitable for the induction of GRP78, the basal, low hARTC1 protein levels were restored. In line with the acute increased levels of endogenous hARTC1, endogenous ADP-ribosylation of GRP78 was also induced by the treatments with DTT (2 mM, 20–120 min) and thapsigargin (1 μM, 20–120 min; as also with thapsigargin 0.3 μM), as detected by far-Western blotting using the *macro* domain (Fig. 8a). Of note, in agreement with previous data [40] and with our data showing that hARTC1 is rapidly down-regulated with

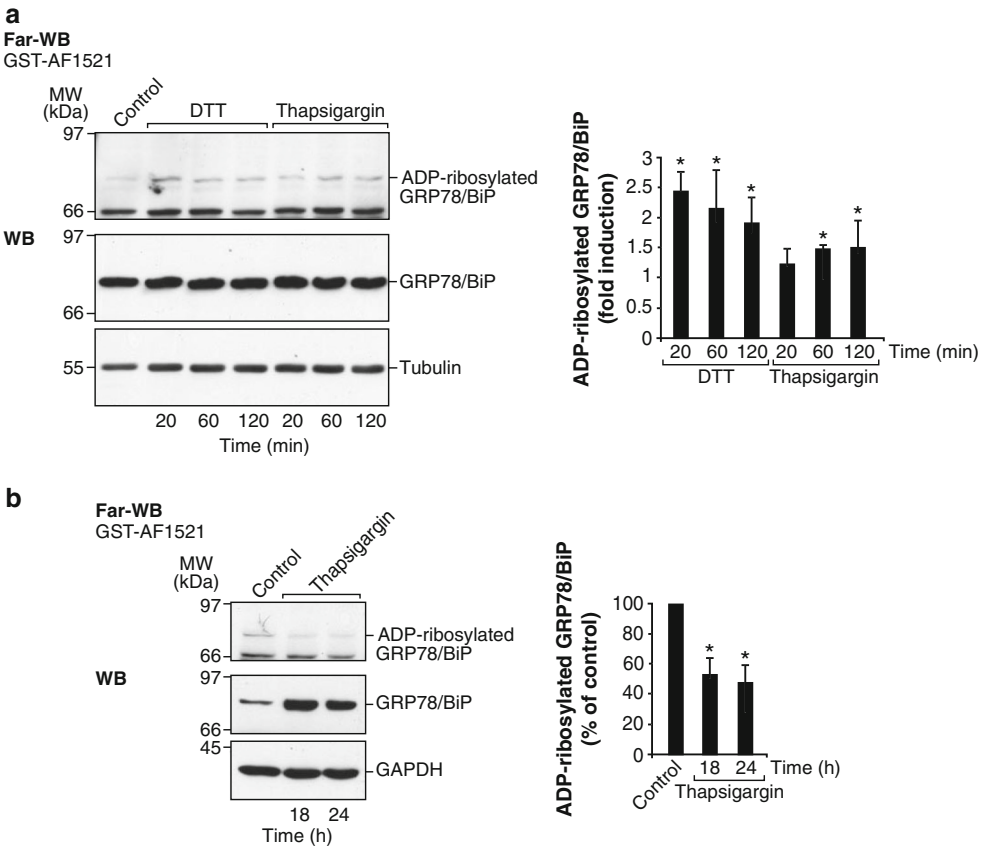

Fig. 8 Representative far-Western blotting (FAR-WB) of HeLa cells not treated (control) or treated for the indicated time with DTT (2 mM) or thapsigargin (1 μM). Solubilised proteins were separated by SDS-PAGE, transferred to nitrocellulose filters, and incubated with GST-tagged *m*Af1521 (see "Methods"). The indicated band (ADP-ribosylated GRP78) was recognised with an anti-GRP78 specific antibody. Data are representative of at least three independent experiments. *Asterisk* significantly different from the relevant control ($p < 0.05$)

longer treatments with thapsigargin (0.3 μM, 18–24 h), longer treatments with thapisgargin were accompanied by reduced staining of the 80 kDa and other protein bands, as evaluated by far-Western blotting with the *macro* domain (Fig. 8b). Thus, the same stressors that have previously been shown to induce ER stress can also induce hARTC1 and ADP-ribosylation of GRP78 with more rapid timing than the activation of GRP78, which suggests that induction of hARTC1 and the consequent GRP78 ADP-ribosylation are the first cell responses to these stress conditions and that they are probably associated with a reduced flow of proteins into the ER.

Discussion

Endogenous mono-ADP-ribosylation is believed to have important roles in cell signalling and regulation; however, identification of the enzymes that are responsible for this intracellular post-translational modification has remained elusive. Here, we report on the characterisation of hARTC1, and we unveil its ER localisation and its modification of the ER chaperone GRP78.

Mono-ADP-ribosylation of GRP78 has been reported previously, with the suggestion that this post-translational modification can regulate the availability of functional GRP78 [38]; indeed, mono-ADP-ribosylation has been detected in response to nutritional stress, and it appears to provide a buffering system that allows the rates of protein processing to be balanced with those of protein synthesis [38]. Despite the physiological relevance of this modification, the enzyme(s) involved have not been characterised to date.

We have previously hypothesised that an enzyme located in the lumen of the ER catalyses this mono-ADP-ribosylation. This is because of the luminal localisation of GRP78, and thus from a topological point of view, this reaction might be catalysed by an ARTC family member [13]. Recently, we discovered that the *macro* domain can be used to bind and pull-down ADP-ribosylated proteins [38]. Performing the *macro*-domain-based pull-down assays, we show here that when either arginine-specific hARTC1 or cARTC2.1 is overexpressed in mammalian cells, this leads to GRP78 mono-ADP-ribosylation. Recently, the Arg470 and Arg492 in the substrate-binding domain of the hamster GRP78 chaperone were mapped as the sites of ADP-ribosylation [41], in line with our demonstration that arginine-specific ARTC1 can catalyse [^{32}P]-ADP-ribosylation of GRP78 (Fig. 5b). It was previously reported that GRP78 oligo- or poly-ADP-ribosylation can

also occur in cells, although to a lower extent as compared to its mono-ADP-ribosylation (4.5 vs. 79 %) [50]. Thus, while the mono-ADP-ribosylation of GRP78 can be induced by the arginine-specific mono-ADP-ribosyltransferase hARTC1, different cellular enzyme(s) can contribute to the ADP-ribosylation of GRP78.

Importantly, here we have further developed the use of the *macro* domain for application in immunofluorescence microscopy, thus allowing visualisation of ADP-ribosylated proteins in intact cells. Using the *m*Af1521, perinuclear staining that co-localised with GRP78 was seen upon cell transfection with the active enzymes hARTC1 and cARTC2.1, but not with their inactive counterparts (hARTC4 and cARTC2.1-E207G/E209G, respectively). Considering that hARTC1 and cARTC2.1 ADP-ribosylate various proteins (Fig. 5a), it is likely that other ADP-ribosylated proteins in addition to GRP78 contribute to this ER-associated *macro*-domain staining. Our results imply that the ARTC substrate NAD^+ is present in the ER possibly also in downstream compartments. This is consistent with previous reports showing that forced expression of the enzymatic domain of PARP1 results in spontaneous formation of luminal poly-ADP-ribose polymers [25].

We have previously shown that cARTC2.1 is well expressed in mammalian CHO cells and that it has high ART activity and localises to cell membranes [25]. Thus, a possible explanation for its modification of GRP78 is its transient presence *en-route* to the plasma membrane, while the absence of detectable peripheric staining with GST-*m*Af1521 can be explained considering that there is not sufficient extracellular NAD^+ to sustain ADP-ribosylation events. Of note, our results indicate that hARTC1 is preferentially located in the ER in transfected cells and that this localisation of hARTC1 is not modified by cycloheximide treatment (Fig. 6a–c); moreover, the 51 ± 2 % of the endogenous hARTC1 co-localises with the ER protein calnexin (Fig. 6d). Although this new finding counteracts the dogma that has asserted that hARTC1 is an ecto-enzyme, it is in line with previous data that have suggested that in rabbit skeletal muscle, 70 % of the ARTC1 activity is localised to the sarcoplasmic reticulum [51]. Moreover, the localisation of the NAD^+ that is required to sustain the ADP-ribosylation reaction in the ER was solved by elegant experiments that allowed the visualisation of an ER-localised NAD^+ pool, by means of the targeted expression of the catalytic domain of poly(ADP-ribose)polymerase (PARP) in the ER [52]. This thus led to the conclusion that all of the components of the machinery for GRP78 mono-ADP-ribosylation (the ARTC and both of the substrates) localise to the ER. In conclusion, we show here that hARTC1 is located in the ER and that it can ADP-ribosylate GRP78. Moreover, silencing of the hARTC1 enzyme reduces the basal level of ADP-ribosylated GRP78, thus providing the direct demonstration that hARTC1 is responsible for the long-known modification of GRP78.

In terms of the biological function of this modification, it has previously been reported that mono-ADP-ribosylation of GRP78 occurs in response to nutritional stress and to environmental conditions that can result in reduced protein synthesis, and thus in a reduced flux of proteins into the ER [38]. Here, we show that endogenous hARTC1 is rapidly induced by acute treatments of cells with the stressors DTT and thapsigargin (Fig. 7a, c) and that this results in increased levels of ADP-ribosylated GRP78 (Fig. 8a). It is possible that this increase in the levels of modified GRP78 are underestimated, considering that ADP-ribosylation is a reversible reaction, and, therefore, the modified GRP78 might become the substrate of a specific hydrolase that can regenerate the non-modified form. Both DTT and thapsigargin are well-characterised inducers of the UPR in human cells, as they affect correct protein folding. Specifically, treatment with DTT results in the ER retention of newly synthesised proteins that cannot fold correctly as they cannot form disulfide bonds [53], while the treatment with thapsigargin inhibits the ER Ca^{2+}-ATPase, thus causing depletion of the ER calcium [54], which is associated with a slowed rate of protein processing. Of note here, both thapsigargin and DTT have been reported to inhibit translation: 10 min treatments are enough to inhibit the synthesis of almost all proteins (see [37] and reference therein). We have also confirmed these data in HeLa cells (not shown). However, mammalian cells can adapt to this translational inhibition: during longer term exposure to both thapsigargin and DTT, for 2–3 h, protein translation is recovered and GRP78 is expressed [54]. Thus, our data demonstrate that acute treatment (from 20 min to 2 h) with the ER stressors DTT and thapsigargin induces mono-ADP-ribosylation of GRP78. In line with previous data [41], we also found that a prolonged treatment with these stressors is not associated with mono-ADP-ribosylation of GRP78. These data thus link the activation of hARTC1 and the ADP-ribosylation of GRP78 to the acute treatments with these ER stressors that have been reported to induce a reduction in the protein flow into the ER, and this is in line with previous observations showing that the ADP-ribosylated form of GRP78 accumulates when protein flow to the ER is decreased. This last is a condition in which the cell does not require the GRP78 activity, which is needed to fold newly synthesised proteins

The interaction of GRP78 with newly synthesised proteins is regulated by the nucleotide (ADP or ATP) bound to the chaperone. The Hsp70 chaperones are characterised by an amino-terminal ATPase domain and by a carboxy-terminal substrate-binding domain. The nucleotide occupancy of the amino-terminal domain of GRP78 controls the

peptide-binding affinity of the carboxy-terminal substrate-binding domain where ADP-ribosylation occurs [41]. According to the current model, the ATP-bound chaperone interacts with a newly synthesised polypeptide through its substrate-binding domain in an open, low-affinity conformation. The ATP hydrolysis then generates the ADP-bound chaperone, which binds polypeptides with high affinity. Then, ADP is released, and the consequent binding of ATP opens the substrate-binding domain, with the release of the polypeptide. Thus, cycles of ATP binding, hydrolysis, and nucleotide exchange regulate this substrate binding and release [55]. Chambers and colleagues showed that GRP78 mutations that mimic the negative charge of ADP-ribose can destabilise the chaperone binding to its substrate without affecting its ability to hydrolyse or exchange nucleotides [41], thus providing evidence that ADP-ribosylated GRP78 is integral but inactive with respect to its binding to polypeptides, a condition that is compatible with the need for cells to rapidly reactivate GRP78. The ER stressors thapsigargin and dithiothreitol initially depress protein synthesis, which makes GRP78 unnecessary; however, when translation is restored, these chemical disruptors also induce the accumulation of unfolded proteins, which is a condition that requires GRP78. A reversible, post-translational modification, such as mono-ADP-ribosylation, will allow the rapid regulation of the activity of GRP78 based on the needs of the cell. Our data demonstrate that short treatments with these ER stressors, thapsigargin and DTT, but not with hypoxia or heat shock (which do not affect translation), upregulates expression of hARTC1 (Fig. 7a, c) and induces the ADP-ribosylation of GRP78 (Fig. 8a). This is in line with the proposed model that suggests that rapid ADP-ribosylation of GRP78 is a way to inactivate the chaperone, and thus to avoid its degradation, which will allow the cell to rapidly reactivate GRP78 through its deribosylation. Intriguingly, hARTC1 is only transiently up-regulated by the ER stressors; indeed, through GRP78 ADP-ribosylation, hARTC1 can lead to the accumulation of the unfolded protein and the loss of the recovery of the cell from the stress, which is a condition that is not compatible with cell survival.

Thus, our data are consistent with the hypothesis that, when the protein load into the ER is reduced, GRP78 is ADP-ribosylated. However, it remains to be defined whether the increased levels of ADP-ribosylated GRP78 can also result in the release of GRP78 interactors, which has been suggested because this modification occurs at the carboxy-terminal substrate-binding domain. If this is the case, then this ADP-ribosylation of GRP78 can also be regarded as a facilitator of the UPR. Altogether, these data place hARTC1 within the ER stress response scenario.

Acknowledgments The authors thank Antonio Tamburro for protein identification by MALDI-MS analysis, Elena Fontana for preparation of Figures, Marco Scardapane for his advice on Statistical analysis and Chris Berrie for editorial assistance. We thank David Ron (University of Cambridege, UK) for providing us the Flag-GRP78 plasmid. We gratefully acknowledge the financial support of the Banca Popolare dell'Emilia Romagna, the Italian Association for Cancer Research (AIRC IG 11652), and the Deutsche Forschungsgemeinschaft (SFB877-A5).

References

1. Althaus FR, Hofferer L, Kleczkowska HE, Malanga M, Naegeli H, Panzeter PL, Realini CA (1994) Histone shuttling by poly ADP-ribosylation. Mol Cell Biochem 138(1–2):53–59
2. de Murcia JM, Niedergang C, Trucco C, Ricoul M, Dutrillaux B, Mark M, Oliver FJ, Masson M, Dierich A, LeMeur M, Walztinger C, Chambon P, de Murcia G (1997) Requirement of poly(ADP-ribose) polymerase in recovery from DNA damage in mice and in cells. Proc Natl Acad Sci U S A 94(14):7303–7307
3. D'Amours D, Desnoyers S, D'Silva I, Poirier GG (1999) Poly(-ADP-ribosyl)ation reactions in the regulation of nuclear functions. Biochem J 342(Pt 2):249–268
4. Schreiber V, Dantzer F, Ame JC, de Murcia G (2006) Poly(ADP-ribose): novel functions for an old molecule. Nat Rev Mol Cell Biol 7(7):517–528
5. Curtin NJ (2012) Poly(ADP-ribose) polymerase (PARP) and PARP inhibitors. Elsevier B.V. http://www.sciencedirect.com/science/article/pii/S1740675712000060. Accessed 29
6. Dani N, Barbosa AJ, Del Rio A, Di Girolamo M (2013) ADP-Ribosylated proteins as old and new drug targets for anticancer therapy: the example of ARF6. Curr Pharm Des 19(4):624–633
7. Haigis MC, Mostoslavsky R, Haigis KM, Fahie K, Christodoulou DC, Murphy AJ, Valenzuela DM, Yancopoulos GD, Karow M, Blander G, Wolberger C, Prolla TA, Weindruch R, Alt FW, Guarente L (2006) SIRT4 inhibits glutamate dehydrogenase and opposes the effects of calorie restriction in pancreatic beta cells. Cell 126(5):941–954
8. Dani N, Mayo E, Stilla A, Marchegiani A, Di Paola S, Corda D, Di Girolamo M (2011) Mono-ADP-ribosylation of the G Protein βγ Dimer Is Modulated by Hormones and Inhibited by Arf6. J Biol Chem 286(8):5995–6005
9. Di Girolamo M, Silletta MG, De Matteis MA, Braca A, Colanzi A, Pawlak D, Rasenick MM, Luini A, Corda D (1995) Evidence that the 50-kDa substrate of brefeldin A-dependent ADP- ribosylation binds GTP and is modulated by the G-protein beta gamma subunit complex. Proc Natl Acad Sci U S A 92(15):7065–7069
10. Leung AK, Vyas S, Rood JE, Bhutkar A, Sharp PA, Chang P (2011) Poly(ADP-ribose) regulates stress responses and microRNA activity in the cytoplasm. Mol Cell 42(4):489–499
11. Scarpa ES, Fabrizio G, Di Girolamo M (2013) A role of intracellular mono-ADP-ribosylation in cancer biology. FEBS J 280(15):3551–3562
12. Corda D, Di Girolamo M (2003) Functional aspects of protein mono-ADP-ribosylation. EMBO J 22(9):1953–1958
13. Di Girolamo M, Dani N, Stilla A, Corda D (2005) Physiological relevance of the endogenous mono(ADP-ribosyl)ation of cellular proteins. FEBS J 272(18):4565–4575
14. Koch-Nolte F, Kernstock S, Mueller-Dieckmann C, Weiss MS, Haag F (2008) Mammalian ADP-ribosyltransferases and ADP-ribosylhydrolases. Front Biosci 13:6716–6729

15. Okazaki IJ, Moss J (1999) Characterization of glycosylphosphatidylinositiol-anchored, secreted, and intracellular vertebrate mono-ADP-ribosyltransferases. Annu Rev Nutr 19:485–509
16. Hottiger MO, Hassa PO, Luscher B, Schuler H, Koch-Nolte F (2010) Toward a unified nomenclature for mammalian ADP-ribosyltransferases. Trends Biochem Sci 35(4):208–219
17. Di Paola S, Micaroni M, Di Tullio G, Buccione R, Di Girolamo M (2012) PARP16/ARTD15 Is a novel endoplasmic-reticulum-associated Mono-ADP-ribosyltransferase that interacts with, and modifies Karyopherin- < beta > 1. PLoS One 7(6):e37352
18. Kleine H, Poreba E, Lesniewicz K, Hassa PO, Hottiger MO, Litchfield DW, Shilton BH, Luscher B (2008) Substrate-assisted catalysis by PARP10 limits its activity to mono-ADP-ribosylation. Mol Cell 32(1):57–69
19. Glowacki G, Braren R, Firner K, Nissen M, Kuhl M, Reche P, Bazan F, Cetkovic-Cvrlje M, Leiter E, Haag F, Koch-Nolte F (2002) The family of toxin-related ecto-ADP-ribosyltransferases in humans and the mouse. Protein Sci 11(7):1657–1670
20. Paone G, Wada A, Stevens LA, Matin A, Hirayama T, Levine RL, Moss J (2002) ADP ribosylation of human neutrophil peptide-1 regulates its biological properties. Proc Natl Acad Sci U S A 99(12):8231–8235
21. Seman M, Adriouch S, Scheuplein F, Krebs C, Freese D, Glowacki G, Deterre P, Haag F, Koch-Nolte F (2003) NAD-induced T cell death: ADP-ribosylation of cell surface proteins by ART2 activates the cytolytic P2X7 purinoceptor. Immunity 19(4):571–582
22. Zolkiewska A, Moss J (1993) Integrin alpha 7 as substrate for a glycosylphosphatidylinositol- anchored ADP-ribosyltransferase on the surface of skeletal muscle cells. J Biol Chem 268(34):25273–25276
23. Okazaki IJ, Moss J (1998) Glycosylphosphatidylinositol-anchored and secretory isoforms of mono- ADP-ribosyltransferases. J Biol Chem 273(37):23617–23620
24. Corda D, Di Girolamo M (2002) Mono-ADP-ribosylation: a tool for modulating immune response and cell signaling. Sci STKE 2002 (163):PE53
25. Stilla A, Di Paola S, Dani N, Krebs C, Arrizza A, Corda D, Haag F, Koch-Nolte F, Di Girolamo M (2011) Characterisation of a novel glycosylphosphatidylinositol-anchored mono-ADP-ribosyltransferase isoform in ovary cells. Eur J Cell Biol 90(8):665–677
26. Shiu RP, Pouyssegur J, Pastan I (1977) Glucose depletion accounts for the induction of two transformation-sensitive membrane proteinsin Rous sarcoma virus-transformed chick embryo fibroblasts. Proc Natl Acad Sci U S A 74(9):3840–3844
27. Haas IG, Wabl M (1983) Immunoglobulin heavy chain binding protein. Nature 306(5941):387–389
28. Bole DG, Hendershot LM, Kearney JF (1986) Posttranslational association of immunoglobulin heavy chain binding protein with nascent heavy chains in nonsecreting and secreting hybridomas. J Cell Biol 102(5):1558–1566
29. Munro S, Pelham HR (1986) An Hsp70-like protein in the ER: identity with the 78 kd glucose-regulated protein and immunoglobulin heavy chain binding protein. Cell 46(2):291–300
30. Lee AS (2001) The glucose-regulated proteins: stress induction and clinical applications. Trends Biochem Sci 26(8):504–510
31. Flynn GC, Pohl J, Flocco MT, Rothman JE (1991) Peptide-binding specificity of the molecular chaperone BiP. Nature 353(6346):726–730
32. Ellgaard L, Helenius A (2003) Quality control in the endoplasmic reticulum. Nat Rev Mol Cell Biol 4(3):181–191
33. Romisch K (2005) Endoplasmic reticulum-associated degradation. Annu Rev Cell Dev Biol 21:435–456
34. Schroder M, Kaufman RJ (2005) The mammalian unfolded protein response. Annu Rev Biochem 74:739–789
35. Ron D, Walter P (2007) Signal integration in the endoplasmic reticulum unfolded protein response. Nat Rev Mol Cell Biol 8(7):519–529
36. Merksamer PI, Papa FR (2010) The UPR and cell fate at a glance. J Cell Sci 123(Pt 7):1003–1006
37. Brostrom CO, Brostrom MA (1998) Regulation of translational initiation during cellular responses to stress. Prog Nucleic Acid Res Mol Biol 58:79–125
38. Laitusis AL, Brostrom MA, Brostrom CO (1999) The dynamic role of GRP78/BiP in the coordination of mRNA translation with protein processing. J Biol Chem 274(1):486–493
39. Leno GH, Ledford BE (1989) ADP-ribosylation of the 78-kDa glucose-regulated protein during nutritional stress. Eur J Biochem 186(1–2):205–211
40. Staddon JM, Bouzyk MM, Rozengurt E (1992) Interconversion of GRP78/BiP. A novel event in the action of Pasteurella multocida toxin, bombesin, and platelet-derived growth factor. J Biol Chem 267(35):25239–25245
41. Chambers JE, Petrova K, Tomba G, Vendruscolo M, Ron D (2012) ADP ribosylation adapts an ER chaperone response to short-term fluctuations in unfolded protein load. J Cell Biol 198(3):371–385
42. Dani N, Stilla A, Marchegiani A, Tamburro A, Till S, Ladurner AG, Corda D, Di Girolamo M (2009) Combining affinity purification by ADP-ribose-binding macro domains with mass spectrometry to define the mammalian ADP-ribosyl proteome. Proc Natl Acad Sci U S A 106(11):4243–4248
43. Neuvonen M, Ahola T (2009) Differential activities of cellular and viral macro domain proteins in binding of ADP-ribose metabolites. J Mol Biol 385(1):212–225
44. Forst AH, Karlberg T, Herzog N, Thorsell AG, Gross A, Feijs KL, Verheugd P, Kursula P, Nijmeijer B, Kremmer E, Kleine H, Ladurner AG, Schuler H, Luscher B (2013) Recognition of mono-ADP-ribosylated ARTD10 substrates by ARTD8 macrodomains. Structure 21(3):462–475
45. Lupi R, Corda D, Di Girolamo M (2000) Endogenous ADP-ribosylation of the G protein beta subunit prevents the inhibition of type 1 adenylyl cyclase. J Biol Chem 275(13):9418–9424
46. Di Girolamo M, D'Arcangelo D, Cacciamani T, Gierschik P, Corda D (1992) K-ras transformation greatly increases the toxin-dependent ADP-ribosylation of GTP binding proteins in thyroid cells. Involvement of an inhibitor of the ADP-ribosylation reaction. J Biol Chem 267(24):17397–17403
47. Lee AS (2005) The ER chaperone and signaling regulator GRP78/BiP as a monitor of endoplasmic reticulum stress. Methods 35(4):373–381
48. Koch-Nolte F, Glowacki G, Bannas P, Braasch F, Dubberke G, Ortolan E, Funaro A, Malavasi F, Haag F (2005) Use of genetic immunization to raise antibodies recognizing toxin-related cell surface ADP-ribosyltransferases in native conformation. Cell Immunol 236(1–2):66–71
49. Glowacki G, Braren R, Cetkovic-Cvrlje M, Leiter EH, Haag F, Koch-Nolte F (2001) Structure, chromosomal localization, and expression of the gene for mouse ecto-mono(ADP-ribosyl)transferase ART5. Gene 275(2):267–277
50. Carlsson L, Lazarides E (1983) ADP-ribosylation of the Mr 83,000 stress-inducible and glucose-regulated protein in avian and mammalian cells: modulation by heat shock and glucose starvation. Proc Natl Acad Sci U S A 80(15):4664–4668
51. Soman G, Mickelson JR, Louis CF, Graves DJ (1984) NAD: guanidino group specific mono ADP-ribosyltransferase activity in skeletal muscle. Biochem Biophys Res Commun 120(3):973–980
52. Dolle C, Niere M, Lohndal E, Ziegler M (2010) Visualization of subcellular NAD pools and intra-organellar protein localization by poly-ADP-ribose formation. Cell Mol Life Sci 67(3):433–443

53. Taniyama Y, Kuroki R, Omura F, Seko C, Kikuchi M (1991) Evidence for intramolecular disulfide bond shuffling in the folding of mutant human lysozyme. J Biol Chem 266(10):6456–6461
54. Thastrup O (1990) Role of Ca2(+)-ATPases in regulation of cellular Ca2+ signalling, as studied with the selective microsomal Ca2(+)-ATPase inhibitor, thapsigargin. Agents Actions 29(1–2): 8–15
55. Bukau B, Weissman J, Horwich A (2006) Molecular chaperones and protein quality control. Cell 125(3):443–451